Chapter 2

Nuts and Bolts: Operational Details of the Caltech Solar Experiment

The Solar Loop Experiment starts with nothing: no gas and no electromagnetic fields. Into this vacuum, the gas and magnetic field are introduced a few milliseconds prior to the experiment. At a precisely timed moment, a large capacitor bank discharges across the electrodes, initiating breakdown of the neutral gas and forming a plasma that lasts less than 10 μs. In this short time window, a set of diagnostics acquire a variety of data such as fast camera images, the plasma current, the electrode voltage, and x-ray emission levels. All of this occurs literally faster than the blink of an eye.

This chapter describes the Caltech Solar Loop Experiment both in setup and in operation. Sec. 2.1 outlines the steps taken to create a plasma, the experimental parameters that can be controlled, and the general plasma behavior. Sec. 2.2 then details the existing diagnostics along with their specifications. These diagnostics include fast cameras, a Rogowski coil, a high-voltage probe, x-ray diodes, and an optical spectrometer.

2.1 Creating the Plasma

This section discusses the steps taken to create the plasma: the injection of neutral gas, the creation of a bias magnetic field, the discharge of the main bank, breakdown, and general plasma behavior. Concurrent with this description, we shall see the different experimental parameters that can be controlled to obtain different plasma behavior. These parameters include the gas species, gas line pressure, gas valve supply voltage, bias field configuration and strength, and main discharge voltage. Different permutations of these parameters yield a wide variety of plasmas to study.

2.1.1 Vacuum Chamber and Plasma Electrode

The Solar Loop Experiment is contained in a large vacuum vessel so that the plasma does not interact with the vessel walls. The chamber is about 1.58 meters long and 1.4 meters in diameter, while the plasma loop is less than twenty centimeters in diameter. Hence, the plasma only interacts with the metallic wall boundary at the footpoint of the loop. This simulates the boundary conditions of a solar coronal loop on the surface of the sun and is distinguished from many other laboratory plasmas that fill up the volume of the vacuum vessel and interact with the vessel walls over large areas. Indeed, the Caltech chamber is so large that the opposite side houses an entirely different experiment, the Caltech Spheromak Experiment. A schematic of the vacuum chamber and all the diagnostics to be discussed is shown in Fig. 2.1.

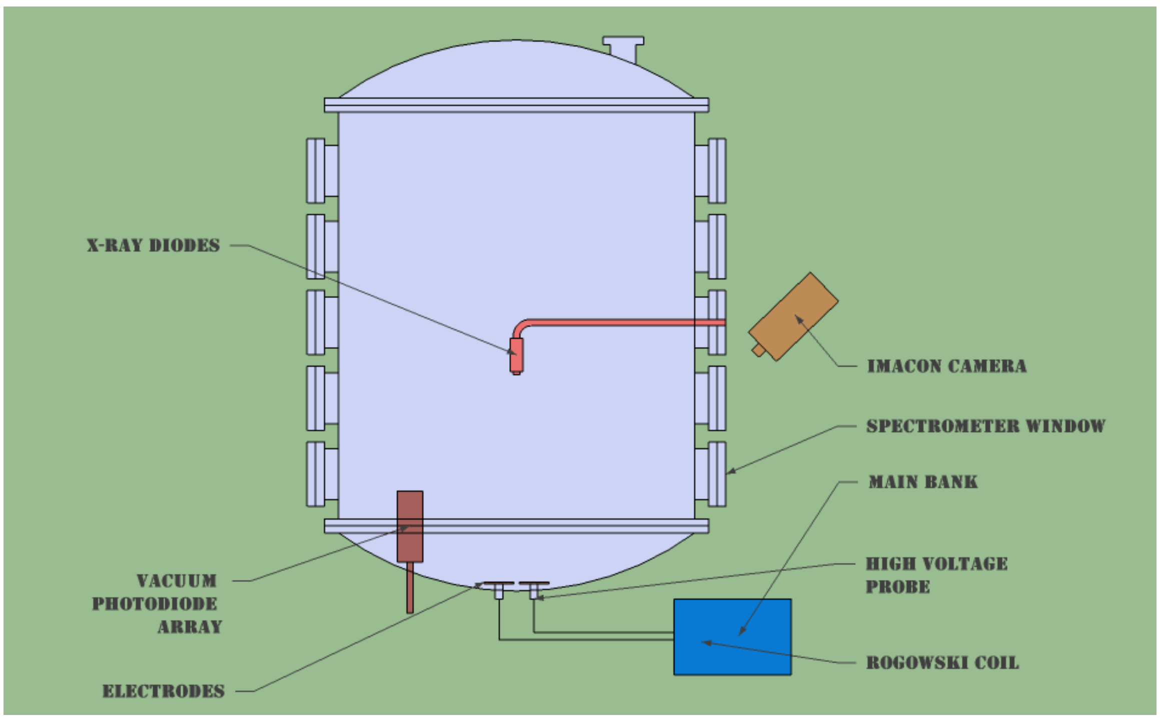

Figure 2.1: A bird's eye view of the vacuum chamber and the positioning of the diagnostics.

The electrodes themselves are copper plates shaped into quarter circles as shown in Fig. 2.2. The top two electrodes are cathodes while the bottom two are anodes. A hole, or gas inlet, in the center of each electrode allows neutral gas to be puffed into the chamber, and coils of wire behind the electrodes generate a magnetic field that links the anode and cathode. The planar nature of the electrodes is based on the Spheromak experiment [18], allowing direct observation of the plasma formation during helicity injection.

2.1.2 Injecting Neutral Gas

The species of gas chosen for the plasma affects the plasma properties through the differences in atomic masses, the number of electrons to contribute to the free electron density, and differences in atomic line emission. The Caltech Experiment is designed with a flexible plumbing system [36, pg. 22] to make switching gas species an easy process. The plasmas studied in this thesis are hydrogen unless otherwise noted, but other options include nitrogen, argon, and deuterium.

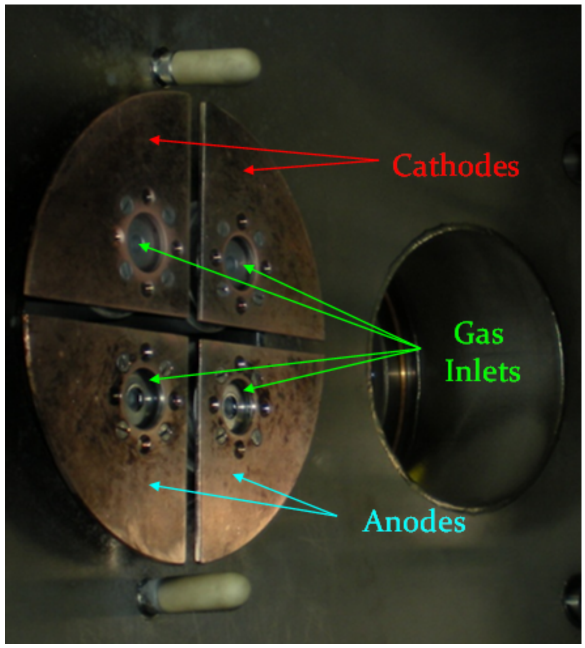

Figure 2.2: The electrodes consist of four planes of copper with gas inlets bored through to allow neutral gas into the chamber.

The vacuum chamber is maintained at a pressure of roughly 10^{-7} torr, and neutral gas is injected into the chamber milliseconds before forming a plasma. This contrasts with many other plasma experiments where the entire chamber is pre-filled at the desired pressure. A fast gas valve separates the vacuum from the reserve of neutral gas, which is typically pressurized from 60 to 100 PSI. The gas valve, designed by Prof. Bellan and shown in Fig. 2.3, consists of a plenum filled with high-pressure gas and a metallic valve held in place by a spring. The spring presses the valve onto an o-ring that maintains vacuum. Milliseconds before the shot, a capacitor bank is discharged into a coil of wire below the valve producing a magnetic field that pushes the valve open against the spring and allows gas to flow for a brief amount of time. The gas in the plenum then travels through a tube at roughly its sound speed to the electrodes. As shown in Fig. 2.2, gas inlets bored through the electrodes allow the gas to expand outward into the vacuum chamber.

The amount of gas admitted by the gas valve can be controlled by adjusting the charging voltage of the gas valve power supply. The amount of gas admitted can be roughly measured by pulsing

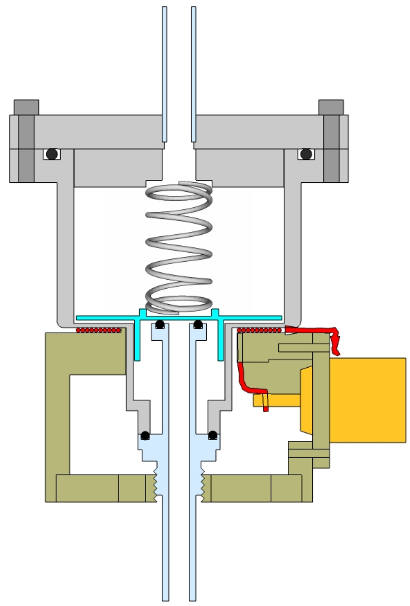

Figure 2.3: A fast gas valve keeps the high pressure gas isolated from the vacuum. When triggered, the valve opens briefly, admitting a small amount of gas.

the gas valve and recording the rise in chamber pressure, which is proportional to the number of particles admitted. The results of this experiment, performed on a smaller test vacuum chamber with valve identical to the ones on the main experiment and using the actual power supply, are shown in Table 2.1 for the three main gas species used. Note that the amount of hydrogen admitted rises rapidly and non-linearly with the charging voltage.

The values reported in Table 2.1 do not necessarily reflect the actual dependence of the plasma density. While increasing the charging voltage of the gas valve power supply lets more gas into the chamber, this higher throughput reflects the total amount of gas that passes the gas inlets integrated over the entire gas puff. What truly matters for the plasma is the instantaneous density of the neutral cloud in front of the electrodes and in the gas inlets at the moment the main bank discharges. The larger values of admitted gas obtained by increasing the charging voltage could be caused by a longer, more sustained gas puff, which would not necessarily provide more gas to the plasma. In order to truly ascertain the instantaneous value of the neutral cloud density, a fast ion gauge should be constructed for the Solar Loop Experiment. We also point out that, on the Solar Experiment, one gas valve feeds *two* gas inlets. The amount of gas admitted and resulting plasma densities will be an important issue in Chapter 4.

Gas Valve Charging Voltage	Hydrogen Pressure	Argon Pressure	Nitrogen Pressure
400 V	21 mtorr	0 mtorr	4 mtorr
450 V	83 mtorr	4 mtorr	11 mtorr
500 V	183 mtorr	10 mtorr	23 mtorr
550 V	436 mtorr	18 mtorr	45 mtorr
600 V	810 mtorr	32 mtorr	74 mtorr
650 V	1314 mtorr	46 mtorr	112 mtorr

Table 2.1: The pressure rise in the small vacuum chamber resulting from a single puff of a fast gas valve as a function of the charging voltage of the gas valve power supply. The hydrogen gas line is pressurized to 100 PSI, while the nitrogen and argon lines are pressurized to 60 PSI; these gas line pressures are used consistently in the experiments presented in this thesis. The amount of hydrogen puffed is a rapidly increasing and decidedly non-linear function of charging voltage. This does not necessarily reflect the density of the neutral cloud at the instant the main bank fires; this must be determined by building a fast ion gauge for the Solar Loop Experiment. On the Solar Loop Experiment a single gas valve feeds two gas inlets.

2.1.3 Bias Magnetic Field

The fast gas valve provides the matter that forms the bulk or "body" of the plasma, but another key ingredient is a background or bias magnetic field to serve as an initial "skeleton" over which the plasma forms. The bias field links the anode to the cathode and is responsible not only for the arched nature of the plasma but also for helicity injection once current flows. The bias field is created by discharging capacitor banks into four coils of wire, each located behind one of the electrode quadrants. The coils are energized 1.7 ms before plasma formation to allow the field time to diffuse through the metal chamber and electrodes. It is important to note that, on the microsecond timescale of the plasma, magnetic fields do not have enough time to diffuse through the electrodes. As the bias field evolves on a millisecond timescale and the plasma lasts roughly ten microseconds, the bias field can be considered stationary over the plasma's lifetime, and the magnetic boundary conditions are essentially "locked in" by the instantaneous value of the bias field when the main bank fires.

The bias field can be modified in two ways. First, the charging voltage of their power banks can be varied continuously, allowing the strength of the magnetic field to be changed. A stronger magnetic field is harder to bend [2, pg. 372], so adjusting the charging voltage allows some degree of control over the rigidity of the plasma. However, the coils are wrapped around iron cores that are saturated by the field. Because of this saturation, the magnetic field is not proportional to the charging voltage but instead varies only weakly with charging voltage in the typical operating regime. Second, one can reverse the polarity of the bias field, which in turn reverses the helicity of the plasma. This can be seen most immediately from Eq. (1.8); reversing the direction of the bias field reverses the sign of the flux Φ and hence the sign of dK/dt. A more intuitive picture will be provided in Sec. 2.1.5. The polarity of the bias field is reversed by switching the hook-ups of the coils to the capacitor banks. Dual-loop experiments may be performed with any combination of field polarities; in particular, both co- and counter-helicity configurations are accessible.

To describe the bias field configuration, we use the following notation. To determine the handedness of each loop, we use the following convention. Point the thumb of your right hand in the direction of the axial magnetic field. If your fingers curl in the same sense as the azimuthal field, the loop is righthanded, and we denote this helicity by the letter R. If the azimuthal field points in the opposite sense of your fingers, the field is lefthanded, denoted as L. Since the azimuthal field is generated by the axial current, the field is automatically righthanded when the current is parallel to the axial magnetic field and lefthanded when the current is anti-parallel to the axial field. As each loop is either right- or lefthanded, we denote the bias field configuration for dual-loop experiments by concatenating "R" or "L" for each loop, the first letter denoting the left loop and the second letter denoting the right loop. The RL and LR configurations are both counter-helicity, while the RR and LL configurations are both co-helicity. These configurations are depicted in Fig. 2.4

We mention in advance that the plasma behaves asymmetrically between the counter-helicity field configurations RL and LR. The cause for this asymmetry has not yet been identified, but, barring asymmetries in the experimental setup, this asymmetry is quite surprising, as MHD predicts that reversing the magnetic field would simply produce a mirror image of the original plasma. This phenomenon, along with fast camera images, is discussed in Sec. 4.4.

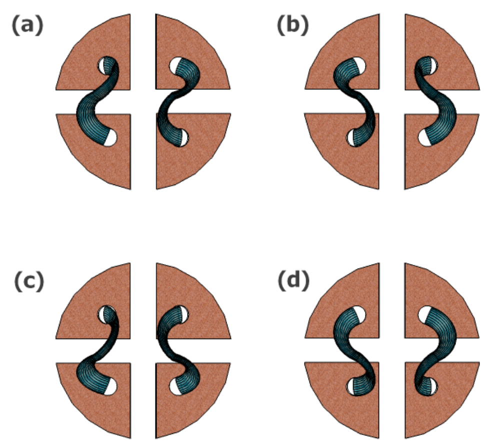

Figure 2.4: Dual-loop experiments can be configured in four different ways: two co-helicity and two counter-helicity. (a) Both loops are right-handed, denoted as RR. (b) Both are left-handed, denoted as LL. (c) The left loop is right-handed, but the right one is left-handed, denoted as RL. (d) The left loop is left-handed, but the right one is right-handed, denoted as LR.

2.1.4 Main Bank

Having admitted gas and established a bias magnetic field, the main capacitor bank then fires, initiating breakdown and bringing the plasma to life. The main bank has a 59 μF capacitor that is switched by an ignitron and is connected to the electrodes by low-inductance cables designed by

Professor Bellan. The bank can be charged up to 6 kV, storing about a kilojoule of electrical energy. When fired, the capacitor first establishes a large potential difference across the electrodes, but current cannot yet flow across the electrodes because the gas has not yet ionized. During this time, free electrons are accelerated by the electric field from cathode to anode along the bias magnetic field lines. These accelerated electrons collide with and ionize neutral gas atoms, creating ions and more electrons. If an electron ionizes several atoms before reaching the anode, we have a multiplication of electrons, also known as an avalanche effect, which leads to full breakdown. At this point, the current begins to flow across the electrodes.

The electrodes have been carefully designed so that breakdown is most favored along the arched path between the gas inlets as opposed to the narrow gap between the electrodes. This is possible due to the Paschen curve, which dictates when breakdown is most likely [1, pg. 227]. The gap between electrodes is so narrow and the gas density there is so low that an electron is unlikely to make any ionizing collisions before reaching the anode. However, later into the shot, arcing is observed between and behind electrodes, presumably because the distribution of gas and plasma has changed.

For the Spheromak Experiment, the main capacitor bank acts as a current source for the plasma after breakdown [37]. This is because the impedance of the ignitron and cables greatly exceeds that of the plasma itself, and we expect similar behavior from the Solar Experiment. However, as will be discussed in Chapter 4, the plasma loops can detach from the electrodes, breaking the conducting path between electrodes. Electrically speaking, the impedance of the plasma load could rapidly change from extremely low to near infinite, and large disruptions are indeed seen in the plasma current. We thus assume that the main bank is a current source with the possible exception of the plasma undergoing a significant change such as detachment.

2.1.5 General Plasma Behavior

Plasma created by the Caltech Solar Loop Experiment can have a variety of behaviors based on the setting of the experimental parameters. There are, however, some general features that are common to most or all plasmas formed by the experiment. These features include twisting, kinking, expansion, and collimation.

The electrodes inject helicity into the plasma loops, inducing twisting and kinking. The twisting can be understood as follows. Current flowing axially through the plasma generates its own magnetic field, different from the bias field, that wraps around the loop in a righthand fashion. The total magnetic field is the vector sum of the bias field and the field generated by the plasma current and is thus helical. The stronger the field generated by the plasma current, the lower the pitch of the helices. The plasma current grows over the course of the shot, and the field lines are thus continually twisting. The plasma, which can be considered frozen to the magnetic field lines [2, sec.

2.6.4], also starts to twist. The kinking of the loop is essentially a version of the Kruskal-Shafranov kink instability [38, 39], which the plasma eventually undergoes due to its increasing current and length. Intuitively, the kinking can be understood by trying to twist a rope or string as much as possible; eventually, the rope tries alleviate the twist by kinking. In the Solar Loop Experiment, the kink gives rise to an apparent central dip in the loops, as shown in Fig. 2.5.

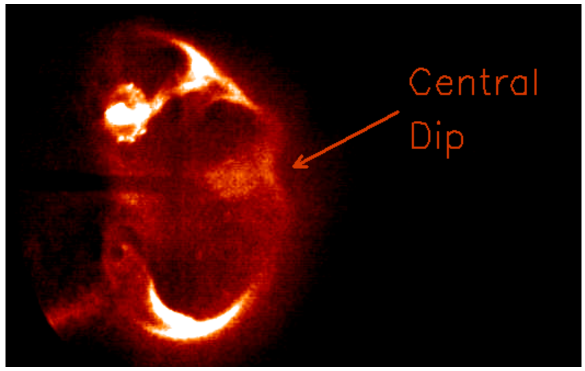

Figure 2.5: A central dip forms in the plasma due to the kinking of the column in response to the increase in magnetic helicity.

The plasma loops expand outward due to the hoop force [2, pg. 311]. The hoop force is a magnetic force that a loop of current exerts on itself; it tends to cause the loop to expand radially. The rate of expansion is influenced both by the plasma current and also by the mass of the plasma as will be shown in Chapter 4. Additionally, it is sometimes observed that the legs of the plasma loop will expand faster than the central region, or that one of the upper or lower legs will expand faster than the other.

The plasmas created are remarkably collimated and remain so throughout the experiment. Similar behavior has been observed in actual solar coronal loops, and an explanation for this universal plasma behavior involves a close look at the MHD forces at work [40], which we outline here. Suppose, for illustrative purposes, that the plasma loops are axisymmetric. Radial equilibrium implies that the radial pressure gradient balances the magnetic pinch force; from Eq. (1.6),

$$\frac{\partial P}{\partial r} = -J_z B_\phi. \tag{2.1}$$

One can integrate and obtain

$$P(r, z) - P(0, z) = -\int_0^r J_z(r', z) B_\phi(r', z) d'r. \tag{2.2}$$

If the plasma loop is bulged and has a radius that varies with axial position, the current density and magnetic field will likewise vary with axial position. The resulting pressure will also depend on z, which results in an axial pressure gradient that pushes plasma towards the bulged region.

This plasma convects toroidal magnetic field into the bulged region, increasing the pinch force and causing collimation. Since the Caltech plasmas are slightly bulged towards the apex where the bias field is weakest, the MHD forces pump plasma from the gas inlets towards the central region from *both* anode and cathode. Such flows have been observed on both the spheromak experiment [41] as well as the Solar Loop Experiment [42, 43].

2.2 Diagnosing the Plasma

A suite of diagnostics are available to study the many aspects of the plasma: fast cameras take pictures of optical emission, the plasma current and voltage are monitored with a Rogowski coil and high-voltage probe, x-ray diodes measure high-energy radiation, and an optical spectrometer provides spectral resolution. The physical layout of all these diagnostics in and around the main chamber is depicted in Fig. 2.1. In this section, we briefly describe each diagnostic as well as the typical uses for their data. The vacuum photodiode array, a new diagnostic, will be described in Chapter 3. Also, modifications made to the current and voltage diagnostics will be discussed in Appendix A.

2.2.1 Fast Camera

The Imacon camera (DRS Hadland Imacon 200, 10 bit dynamic range, 1200 x 980 pixels) is a multiframe, high-speed intensified CCD camera suitable for taking optical images of the plasma. The Imacon consists of eight individual cameras each capable of taking two frames per shot. Unfortunately, one camera is not working, so the images presented here have only fourteen frames. The timings of these frames can be programmed to almost any desired timing sequence. Comparing Imacon images from different shots, the plasma is seen to be highly reproducible. The Imacon is typically located at a side viewport, as indicated in Fig. 2.1, but can be moved to almost any window.

The Imacon images are invaluable for determining the position and overall state of the plasma. Certain quantities such as the expansion speed can be estimated from these images, and major events such as detachment from the electrodes can also be seen and hence timed. Imacon images also reveal inhomogeneity in relative brightness of the plasma and readily identify peculiar optical activity such as the bright spot described in Sec. 1.4.1. However, a significant amount of plasma activity occurs in the ultraviolet or x-ray regime that is missed by the Imacon photos. For instance, at late times the Imacon images show that the plasma has detached and drifted far away from the electrodes, but the current trace shows a large current flowing through the electrodes at this time, and the radiation diagnostics shows significant radiation levels. The Imacon camera provides a great deal of information but does not tell the complete story.

2.2.2 Plasma Current and Voltage

The current flowing through the plasma is a fundamental quantity; it determines the toroidal magnetic field, which pinches the plasma radially against the internal pressure, and is a crucial ingredient of the MHD pumping force described in Sec. 2.1.5, which depends the square of the current. A Rogowski coil [2, pg. 245] is used to measure the plasma current. A Rogowski coil is a toroidal solenoid that surrounds a current-carrying wire; the magnetic field from the wire links the turns in the coil and induces a voltage proportional to the time derivative of the current. This signal is passed through an RC integrating circuit, as shown in Fig. 2.6, whose output is then proportional to the original current. The Rogowski coil is placed around one of the capacitor electrodes in the main bank, as indicated in Fig. 2.1. The integrated signal is passed to a optoelectric converter that transmits the signal to the data acquisition device (DAQ). Appendix A contains a discussion of the optoelectric converters and noise issues related to the current measurements.

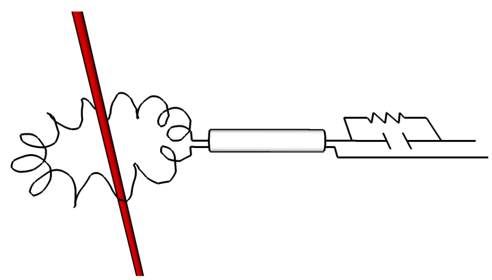

Figure 2.6: A Rogowski coil, shown on the left, encircles a wire, shown in red, and produces an output voltage proportional to the time derivative of the current. The output is fed into a passive RC integrator, shown on the right.

Another important electrical property of the plasma is the voltage across the electrodes. This voltage is a combination of the Ohmic voltage drop and the inductive voltage drop due to the change in the flux linking the plasma:

$$V = IR_p + \frac{d\Phi}{dt} = IR_p + \frac{d(L_p I)}{dt}, \tag{2.3}$$

where R_p is the plasma resistance and L_p is the plasma inductance. As the plasma inductance is strongly related to the plasma loop geometry, sudden jumps in the voltage are indicative of sudden changes in the loop geometry and, perhaps, magnetic field topology as well. For instance, if the plasma loop detaches from the electrode, one would expect the voltage to rise sharply in attempt to maintain the current flow and sustain the enclosed flux.

The voltage is measured using a Tektronic P6015 high-voltage probe clipped to the upper right aluminum clamp that connects the capacitor bank cable to the electrode. Like the output of the Rogowski coil, the voltage signal is transmitted to the DAQ by optoelectric conversion. A number of modifications were made to the probe and the accompanying electronics; for instance, the ground clip of the probe was attached to the lower electrode to improve voltage measurements. These modifications are detailed in Appendix A.

Fig. 2.7 contains a generic example of current and voltage data and provides an overview of the plasma evolution. When the main bank first fires, the voltage increases sharply but current does not yet flow because the plasma is not ionized. The duration of this period depends on several factors such as the amount of gas injected into the chamber and the discharge voltage. At some point, the plasma fully breaks down, resulting in a sharp drop in voltage and the beginning of the current flow. Simultaneously, spurious oscillations associated with the main bank firing and the ignitron switching appear in the current data; these oscillations are discussed in Appendix A. As mentioned above, the change in plasma geometry (in this case, plasma formation) is associated with a sharp change in voltage. The main bank then acts more or less as a current source, and the current trace strongly resembles damped oscillation characteristic of an LCR circuit. The behavior of the voltage trace depends strongly on the plasma itself; in general, though, rapidly expanding plasmas tend to maintain a higher voltage because of the faster rate of change of flux through the plasma loop. The timescale of this plot is selected to show the full discharge; the plasma, however, typically only lasts about 10 μs at most.

2.2.3 X-Ray Diodes

A set of four International Radiation Detector Corporation AXUV-HS5 x-ray diodes monitor soft x-ray levels. The diodes are placed inside the vacuum chamber because the soft x-rays will not transmit through the viewports of the chamber [36, pg. 104]. The diodes are thus affixed to the end of a support arm inside the chamber and look head-on at the electrodes, as shown in Fig. 2.1.

The yield of a bare x-ray photodiode is shown in Fig. 2.8 and is about 1 electron per photon at photon energies of 10 eV. The yield increases by about 17% per 1 eV increase in photon energy. In the set of diodes installed on the Caltech chamber, one diode is bare, while the other three have filters in front of them. The filters are a 200 nm thick sheet of aluminum, which transmits 15-62 eV photons, a 50 nm sheet of titanium, which transmits photons of wavelength less than 15 nm (energies greater than 83 eV) photons, and a 500 nm sheet of titanium, which transmits energies greater than 200 eV. The transmission curves for these filters can be calculated at Ref. [44] and are plotted in Fig. 2.9. No signal has been observed through the 500 nm Ti filter, so that the x-rays produced in the Caltech experiment have energies less than 200 eV per photon. Note that hydrogen lines, whose energies are less than 13.6 eV per photon, are not transmitted by any filter. Thus, a signal registered by the filtered x-ray diodes for a hydrogen plasma is caused by something other than line emission.

The x-ray diodes are extremely fast; their time resolution is enhanced by back-biasing the diodes in order to reduce their parasitic capacitance, allowing them to register very fast x-ray bursts. Their primary limitation is that they have a single line of sight and thus cannot determine from where in the plasma the x-rays originate. Also, due to the construction of the diodes' support arm and their large distance to the electrodes, slight variations in the diodes' inclination angle drastically change the direction of their line of sight. It is perhaps these two issues that introduce large variations in the x-ray diode signals discussed in Sec. 1.4.1. When an x-ray burst is not observed, it is not clear whether the plasma did not emit x-rays or the detectors simply missed the burst. The array of vacuum photodiodes was constructed to address these types of questions.

2.2.4 Spectrometer

The spectrometer measures the relative intensities of different wavelengths of light in a small spectral window. The spectrometer consists of a diffraction grating, which disperses light at different angles according to wavelength, and a CCD camera, which registers the incident radiation. The intensity of light upon a particular CCD pixel is indicative of the number of photons at the corresponding wavelength. This intensity is not calibrated absolutely, but the relative intensity within a spectral window is very accurate. A twelve-channel fiber optic bundle carries the plasma light from the chamber to the spectrometer located across the room. The input to the fiber array is placed outside a viewport of the vacuum chamber as indicated in Fig. 2.1, and each channel views a different spatial chord through the plasma. Light from the plasma enters the fiber optic cables and is transmitted to the spectrometer. The CCD camera can measure each channel independently and simultaneously, providing spectroscopic data from twelve different chords through the plasma.

Spectroscopic data have many different uses, but in this thesis they will be used to estimate the electron density by measuring the Stark broadening of the Balmer H_β line. This technique has been previously utilized on the Spheromak Experiment [45, 36]. For light-emitting hydrogen atoms in a plasma, the local electric field created by the surrounding electrons and ions broadens the spectral line according to the formula [36, pg. 75]:

$$w_s = 2.5 \times 10^{-14} \alpha_{1/2} n_e^{2/3}, \tag{2.4}$$

where n_e is the electron density in m^{-3}, w_S is the width of the H_β line in nanometers with instrumental and Doppler broadening subtracted out, and α is the so called half-width [36, pg. 78]. The spectrometer can also detect the presence of impurities in the plasma and determine their ionization state. If multiple lines are present in the same spectral window, the ratio of the lines can give some indication of the electron temperature under the assumption of local thermodynamic equilibrium. Finally, spectral data can also indicate the speed of a plasma via the Doppler shift of the atomic lines, although this technique will not be employed in this thesis.

The spectrometer's CCD camera opens for a single time window during a shot, and the spectrometer's output is an integration of data over this time window. The duration of the time window is limited by the requirement of receiving enough light to distinguish the signal from the noise. Measurements of the H_β line typically require a gating period of 0.5 μs. The spectral window observed by the CCD camera is typically 4 - 5 nm wide [36, pg. 40]. Although the spectrometer is sensitive from 200 - 500 nm, the lower wavelength limit is actually set by the transmittance of the port windows on the vacuum chamber. Special windows were custom-made out of boroscilicate [36, pg. 104] which will start to attenuate light somewhere between 350 - 400 nm.

2.2.5 Data Acquisition

The data acquisition is handled by fast digitizing boards (SiS GmbH SIS3300) mounted on a VME crate. The boards sample data at 100 MHz, giving a 10 ns time resolution. There are twelve boards with eight channels each for a total of 96 synchronized channels. Every channel has a built-in 50 Ω termination for impedance matching to 50 Ω cables. The dynamic range is ± 0.5 V, and data beyond this range will be clipped. The VME crate is electrically connected to the vacuum chamber though the building ground, and this has important implications for diagnostics using the DAQ. As the ground of the VME crate is connected to the chamber and also to the ground of any diagnostic cable plugging into it, any additional contact between the diagnostic ground and the chamber will result in a ground loop, as is discussed in more detail in Sec. 3.3.2. The crate is powered by an isolation transformer so that it does not additionally couple to ground through its power cord.

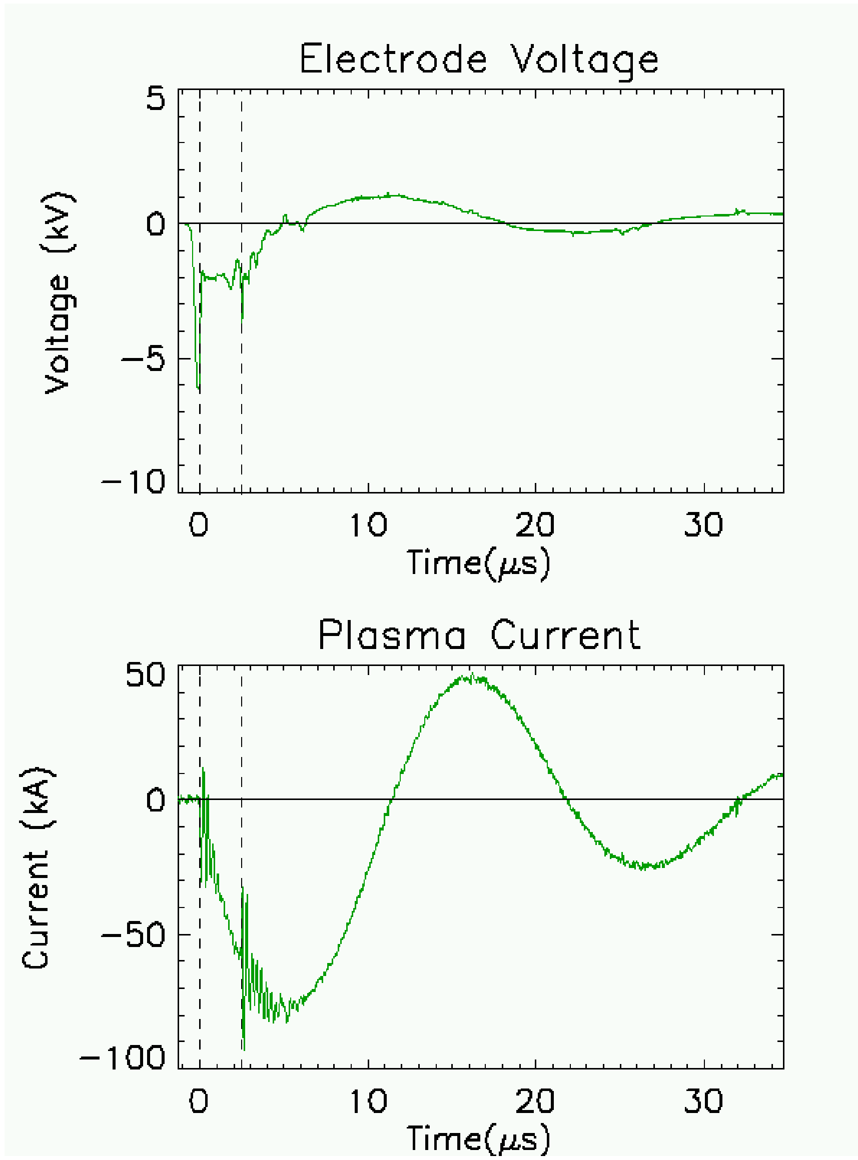

Figure 2.7: The electrode voltage (top) and plasma current (bottom) for a counter-helicity hydrogen plasma (shot 8205). The data are plotted until 35 μs to show the RLC-like ringing of the current, but the main plasma activity occurs most before ~ 8 μs. The leftmost horizontal line is at 0.0 μs, the time at which the plasma breaks down, at which time the voltage plummets while the current starts to flow. The rightmost vertical line is at 2.5 μs. At this time the voltage spikes. At both vertical lines, large oscillations appears on the Rogowski coil. These oscillations are believed to be spurious electrical pick-up; see Appendix A. The voltage spike is, perhaps, indicative of rapid changes in magnetic field topology which result in electrical noise such as the oscillations seen on the current channel.

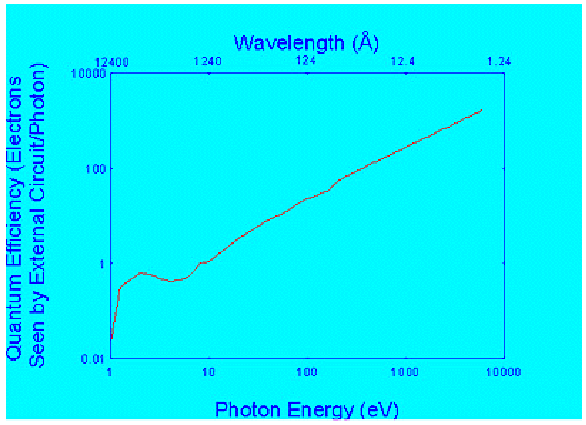

Figure 2.8: The yield, or quantum efficiency, of a bare AXUV-HS5 diode shows that the diodes have a much more favorable response to higher-energy photons.

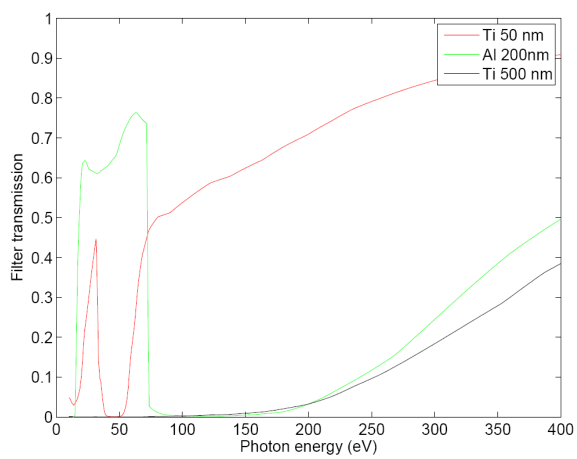

Figure 2.9: The transmission curves for the filters used on the x-ray diodes roughly complement each other is the energy range 10 - 200 eV. The transmission curves are obtained from Ref. [44].